Modeling and simulating a hybrid winds and photovoltaic stand-alone generating systems.

Divyam saxena, Raghvendra Singh, Samir Kumar Mishra

Faculty of Engineering, Rama University Uttar Pradesh Kanpur 209217, India
Email id: dsaxena7798@gmail.com

Abstract:

The primary goal of this research is to simulate and evaluate a Standalone wind-PV Hybrid generating systems using the MATLAB/SIMULINK framework. The investigation will be conducted under various scenarios. The system that is suggested comprises two green energy, namely solar and wind power. The explanation of the modelling of the PV array and wind turbine is concise and easy to understand. It functions as an uninterrupted power supply that can provide a specific minimum quantity of electricity to the load regardless of any circumstances. Power transfer involved many modes of operation, including a standard mode that does not require the usage of a battery, resulting in an intuitive user interface. The control plan manages the electrical power produced by every element to ensure that the combined system operates according to the intended methods of operations. The two systems are integrated to function simultaneously, with the shared DC bus gathering the overall energy generated by the wind and photovoltaic subsystems. This energy is then divided, with a portion used to charge the batteries and the remainder powering the DC load. This work presents a practical wind-PV hybrid framework that can be utilized to analyze the effectiveness of them.
Keywords: MATLAB/SIMULINK, DC load, wind-PV hybrid framework

1.0 Introduction

The increasing utilization of petroleum and coal and the environmental issues linked to them have garnered global focus on energy from alternative sources. Due to the rising demand for electricity and the urgent need to address global warming, there is a growing interest in adopting environmentally friendly energy solutions to protect the Earth for future generations. In addition to hydro power, wind and photovoltaic energy are among the most promising energy alternatives for meeting our energy needs. While several technologies, such as fuel cells, have reached an advanced degree of development.

These power plants have garnered significant attention worldwide. The incorporation of renewable energy sources and energy-storage systems has emerged as a prominent trend in power-electronic technology. The world's rapidly expanding energy resources, a pristine and efficient contemporary technology that offers promise for a future founded on sustainable, environmentally friendly technology. In light of the growing quantity of renewable energy

4373

sources, it is necessary to develop fresh approaches for their operations to uphold or enhance the stability, quality, and dependability of power supply. Today's solar and wind turbines represent the pinnacle of modern technology, as they are modular and can be installed rapidly. The utilization of many renewable energy sources is more advantageous than a single source system in terms of cost, efficiency, and reliability. The prevalent varieties of AC generator utilized in contemporary wind turbine systems are as listed below: The paper selects the variable-speed directly-driven multi-pole permanent magnet synchronous generator (PMSG) wind architecture over the squirrel-cage rotor induction generator. This choice is based on the PMSG's superior performance, which includes higher efficiency and lower maintenance requirements due to the absence of rotor current. The types of generators mentioned include the Wound-Rotor Immersion Power source, DoublyFed Immersion Power source, Asynchronous Generator with external field excitation, and Permanent Magnet Synchronous Generator [3]. PMSG can be utilized independently of a gearbox, resulting in a decrease in the weight of the nacelle and a reduction in costs [3].A standalone wind/PV hybrid generation system provides a viable solution for generating power in remote areas where there is no access to utility networks. Additionally, it is devoid of pollution, which enhances its appeal. In remote areas, a viable method for achieving self-sustaining power generation is to employ a combination of a wind turbine and PV system, along with battery storage, to establish an independent hybrid system [3, 4].

A photovoltaic (PV) system is a straightforward and dependable method for generating electricity by converting solar energy. The fundamental component of a solar photovoltaic (SPV) system is the SPV cell. The output of a Solar Photovoltaic (SPV) system can either be directly connected to the loads or can be utilized through a power electronic converter to optimize its operation at the greatest power point. The numbers 7 and 8. Every of the two components, the PV subsystem plus the wind component, is independently controlled by its own controller. Each controller will direct its respective system to monitor and optimize for the highest power output [6, 7].

The goal of this article is to furnish readers the crucial details for constructing turbine simulators with PV panels which may be employed in simulating a self-sufficient wind/PV generation system, as well as for doing additional research on such systems. This study provides a comprehensive analysis of the equations that constitute the wind turbine and PV panel. The two systems are integrated to function concurrently. The primary objective of this research is to construct a model for simulation of an independent hybrid generating system that incorporates both wind and PV subsystems using the MATLAB/SIMULINK technology. The functional features of the modeled wind generator and solar PV panels are already demonstrated for various circumstances.
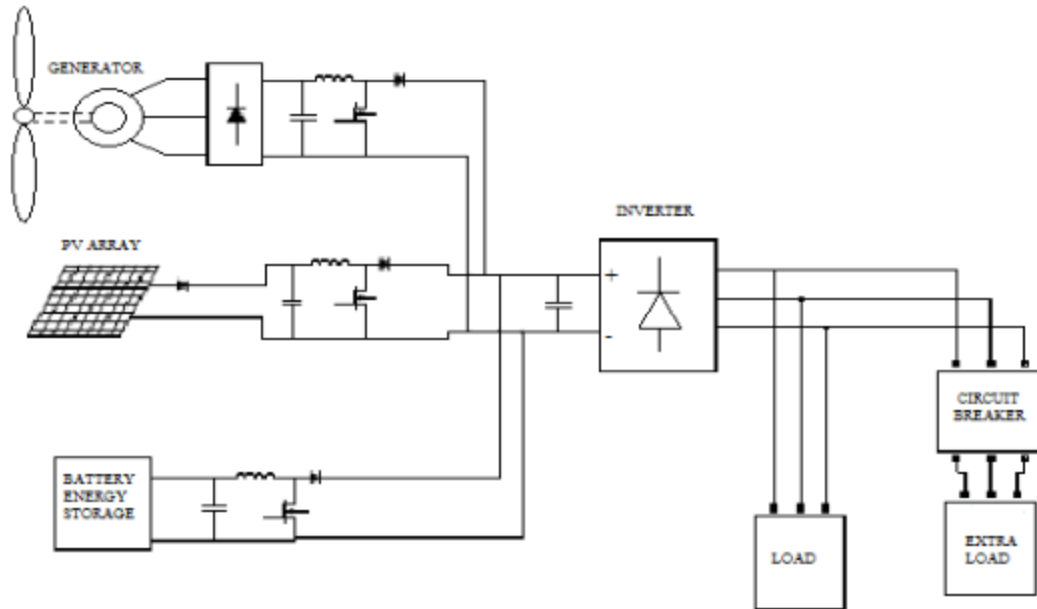
2.0 Proposal Hybrid energy systems

Figure 1 illustrates the set up of hybrid electrical systems.

A. Wind Energy Source The turbine that generates electricity uses a rotor made up of a minimum of two blades that are mechanically linked to an electrical motor to absorb the movement energy of the winds. The calculation expresses the mechanical energy generated from rotor by a turbine that generates wind and can be written as:

$$P_m = 0.5\rho A C_p V^3 \qquad (1)$$

The angle of pitch denotes the inclination at which the wind turbine's blade are oriented in relation to its longitudinal axis. The greatest conceivable value of the strength characteristic Cp is 0.59. The outcome relies on two factors, namely the tip speed ratio (TSR) and the pitch angle. The term TSR, or Tip Speed Ratio, refers to the ratio between the linear speed of the rotor and the speed of the wind.

$$TSR = \lambda = \frac{\omega R}{V} \qquad (2)$$

The aerodynamics tension Tw in N-m can be calculated by dividing the energy obtained from the breeze by the turbine's spin velocity ww in rad/s.

$$Tw = Pw/ Ww$$

The amount of mechanical force transferred to the power plant is equivalent to the plane's aerodynamic acceleration, as there's no gearbox present. The coefficient of power Cp achieves a maximum value of 0.593, indicating that the power obtained from the wind is consistently below

4375

59.3% (Betz's limit) due to the influence of rotor architecture and associated hydrodynamic inefficiencies [8, 9].

Figure 2 displays a standard "Cp vs. λ" graph for a wind turbine. The attainable upper limit of Cp in practical designs varies between 0.4 and 0.5 for high-speed turbines, and between 0.2 and 0.4 for slow-speed turbines. Figure 2 demonstrates that the variable Cp reaches its highest value (Cpmax) at the optimal wavelength (λopt). The windmill captures the most energy and achieves best efficiency from the wind. Figure 3 illustrates the relationship between the output power of a wind turbine and the rotor speed, while the wind speed varies from v1 to v4 (with v4 being greater than v3, v2, and v1). Figure 3 demonstrates that when the speed is v1, the greatest power can be harnessed at a rotor speed of ω1. As the speed increases from v1 to v4, the rotor speed for the full tracking of power points rises as well in ω1 to ω4.
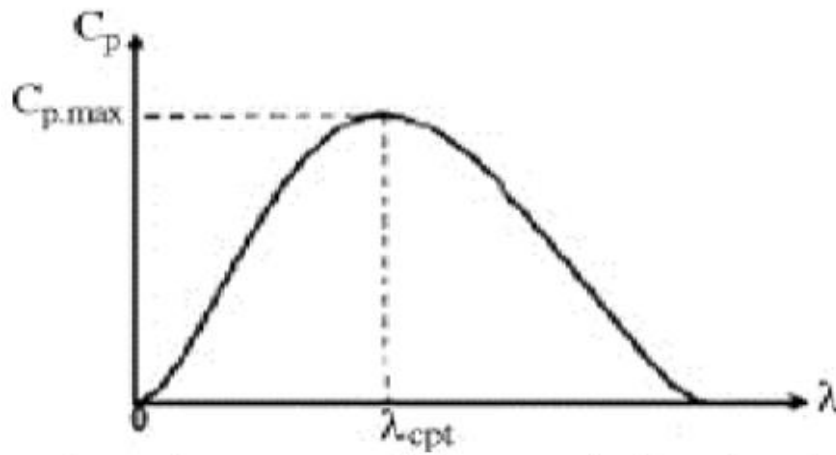

Figure 2 displays the connection between the power coefficients and the tip velocity ratios.
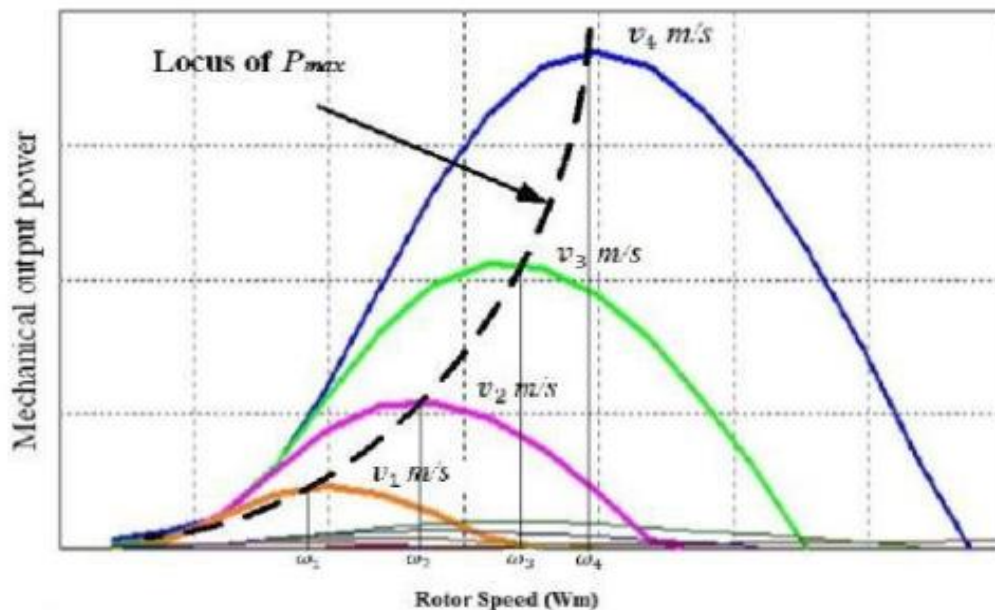

Figure 3 displays the relationship between the output power and rotor speed for multiple speeds.

B. Photovoltaic (PV) System

A cell made from sunlight is the primary and essential element of a photovoltaic, or PV, systems. The PV array is assembled using many photovoltaic cells that have connections in either parallel or series in order to achieve the desired voltage, voltage, current, and high output of electricity [10]. The solar cell can be represented by an analogous circuit consisting of a current source connected parallel with a diode that is biased in the forward direction. Every solar cell resembles a diode, consisting of a p-n junction created by semiconductor material. Each output power characteristic curve exhibits a distinct maximum power point. Figure 5 displays the current-voltage (I-V) and power-voltage (P-V) characteristics of the photovoltaic (PV) array under varying sun intensities. The absorption of light by the connection can generate electric currents through the process known as photovoltaic. The energy output characteristics for the photovoltaic (PV) array in a given solution are depicted in Figure 4. The circuit's output connections are linked to the loads. The present equation describing the solar cell is as follows:

$$I = \bar{I}_{Ph} - \bar{I}_D - I_{sh} \qquad (3)$$

$$I = I_{ph} - I_0 \left[exp \left(\frac{qV_D}{nkT} \right) \right] - \frac{V_D}{R_{SH}} \qquad (4)$$
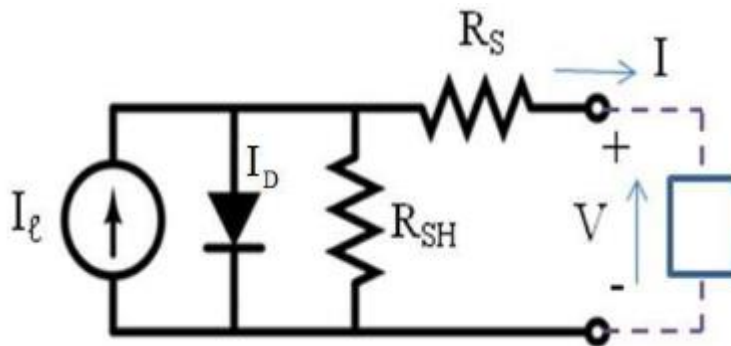

Figure 4 illustrates an analog circuitry of Photovoltaic (PV) Modules.

The electrical power generated of a photovoltaic cell is determined because
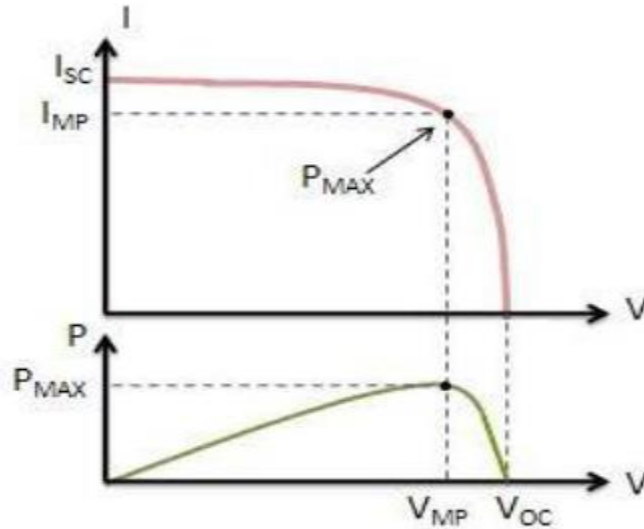
$$P_{PV} = V * I \qquad (5)$$

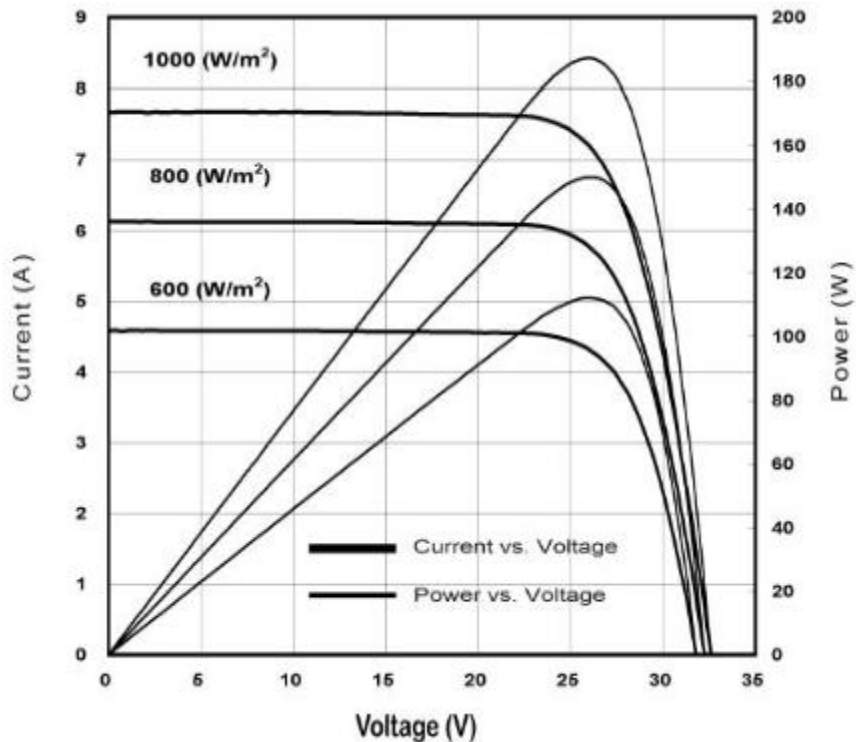Figure 5 depicts the output parameters of the PV Arrays.

Figure 6 illustrates both the I-V and P-V features of a PV array under varying sun intensity.

C. Battery Energy Storage: Batteries for energy storage (BESS) consist of battery packs, a controller, and powered electronics that facilitate the conversion between oscillating and direct current. Different kinds of battery possess distinct benefits as well as drawbacks with regard to of their power and energy capacities, dimensions, mass, and expenses. The primary battery energy storage technologies include Lead-Acid, Nickel Cadmium, Sodium Sulfur, Nickel Metal Hydride, and Lithium-ion batteries Lead-Acid electrodes attain elevated discharge rates through the utilization of deep-cycle battery packs. In summary, Lead-Acid batteries present a

competitive option for energy storage applications due to their low maintenance needs and comparatively low discharge themselves rates. The batteries transform electrical power into chemical energy that is used for the purpose of storage. Batteries undergo charging and discharging processes with direct current (DC) power. The flow of electricity between battery and electrical systems is controlled by bi-directional power electronic devices. Sodium Sulfur batteries exhibit a notable energy density, a commendable charge/discharge efficiency, and a prolonged cycle life. The dominating use of urban renewable energy systems is constrained by low energy density, non-environmentally friendly electrolyte, and a very short life-cycle [16]. Nickel Cadmium (NiCd) batteries surpass Lead-Acid batteries in terms of energy density, cycle life, and maintenance needs. However, these batteries possess the hazardous characteristic of containing cadmium and exhibit higher self-discharge rates compared to Lead-Acid batteries. In addition, NiCd batteries can be significantly more expensive than Lead-Acid batteries, with costs that can be up to ten times higher [17], making them a considerably costly option. Nickel Metal Hydride (NiMH) batteries are small and lightweight, making them suitable for use in hybrid electric vehicles and communications applications. As stated in reference [18], batteries made of NiMH have the ability to replace NiCd batteries in communication devices. In addition, these batteries offer comparable cycle life properties, are eco-friendly, and can deliver an extra capacity of 25 to 40% [18]. They are presently utilized in cellular phones, laptops, and other devices. Furthermore, the advancement of this technology is employed in decentralized applications for storing energy. However, the technique is hindered by its high cost [19] and restricted range of applications. Due to the rapid advancements in lithium-ion technology, it has become the dominant force in the electronics sector. Lithium-Ion technology possesses the greatest energy density compared to all other battery types [19]. Due to its various dimensions, it is utilized in renewable energy systems of small, medium, and large scales. During linked operation, fluctuations in wind and solar PV generation will result in instantaneous adjustments to the output of the Battery Energy Storage System (BESS), which must rapidly counteract these changes in power output. Rate variation control, also known as ramp rate control, is a method used to mitigate changes in real power from a connected system. The Battery Energy System controller processes the information to estimate the state of charge (SOC) and capacity of each battery cell. It also ensures that all the cells function within the designated SOC range. The state of charge (SOC) is a measure of the remaining electrochemical energy in a battery. Utilities often specify the permitted ramping rates in kilowatt per second (kW/min) in wind and solar power purchase agreements with independent power providers. SOC mostly arises because to variations in chemical and electrical properties resulting from the production process, aging, and ambient temperatures. When the state of charge (SOC) is not regulated, for example by cell equalization, the energy storage capacity experiences a significant drop. The State of Charge (SOC) information is subsequently utilized to regulate the charge equalization process. The value is represented as a percentage relative to the total battery capacity. The electrochemical chemistry occurring within batteries is highly intricate and challenging to accurately simulate using electrical models. The concept of SOC is elucidated in references [12] and [13]. Therefore, it is

imperative to implement charge equalization in order to minimize the discrepancies between the battery cells and prolong the overall battery lifespan. Typically, it is recommended to maintain the State of Charge (SOC) of a battery from thirty percent to seventy percent in order to maximize its lifespan.

3. MPPT (A maximum Power Point Tracking)

The maximum energy point tracking approach is employed to enhance the efficiency of both the solar panel and wind turbine by optimizing their operation at the moment of highest power. Various methodologies have been devised and deployed for maximum power point tracking (MPPT) technologies. The output powers of the two systems are measured and compared. If this power is not equal to their maximum powers, then their original reference values are increased or decreased by one increments. Some of the often used approaches include Perturb and Observe (a method based on hill climbing), Incremental Conductance method, Fractional short circuit current, Fractional open circuit voltage, Neural networks, and Fuzzy logic. The aforementioned stages are iterated until the wind turbine and solar array reach their maximum power points. Figure 5 displays the distinctive power curve of a photovoltaic (PV) array. The MPPT technique relies on the initial reference rotor speed for the wind turbine and an initial reference voltage for the solar array. If this modification results in a rise in their output capacities, then the subsequent modification is done in the same direction, and conversely. The issue addressed by MPPT approaches is the automatic determination of the voltage VMP or current IMP at which a PV array should run in order to achieve the highest possible power output PMAX, given particular temperatures and irradiation.

4. Hybrid Power Plant-Wind Systems

Figure 7 depicts the system that is suggested comprising a turbine that generates electricity, a variable velocity direct-drive wind power source, a wind side ac/dc conversion, a solar array, dc/dc converters, and an identical dc load connected together with the battery. A wind turbine harnesses mechanical energy to drive the wind generator, which produces alternating current (AC) electric power. This electricity is then transformed into direct current (DC) power to create the common DC link. The photovoltaic array produces direct current (DC) power with a voltage range of 6 to 7 volts. Each of the two subsystems, the PV component and the wind subsystems, is autonomously regulated by its own controller. Every controller will direct its respective system to monitor the maximum power [6, 7, 18].The system's power output is contingent upon the prevailing meteorological circumstances, such as wind and sun, as well as the battery's state of charge. It is capable of being tested for various system processes.

The control method implemented in this case regulates the battery state of charge by maintaining the DC bus voltage at the specified battery voltage of 48V.The wind subsystem consists of a 480 W wind generation that comes with a direct powered permanent-magnetic synchronous turbine (PMSG), a diode rectifier, and a (DC/DC) buck conversion. The buck converter is used to track the point of greatest power.

A 420 W photovoltaic panel is utilized, with its variable DC output voltage regulated by a separate DC/DC buck converter employed for maximum power point tracking (MPPT). The

shared DC bus accumulates the combined energy generated by the wind and photovoltaic subsystems, allocating a portion to charge the battery and the remainder to power the DC load. Figure 7 depicts the schematic of a simulated autonomous combination PV the wind systems.
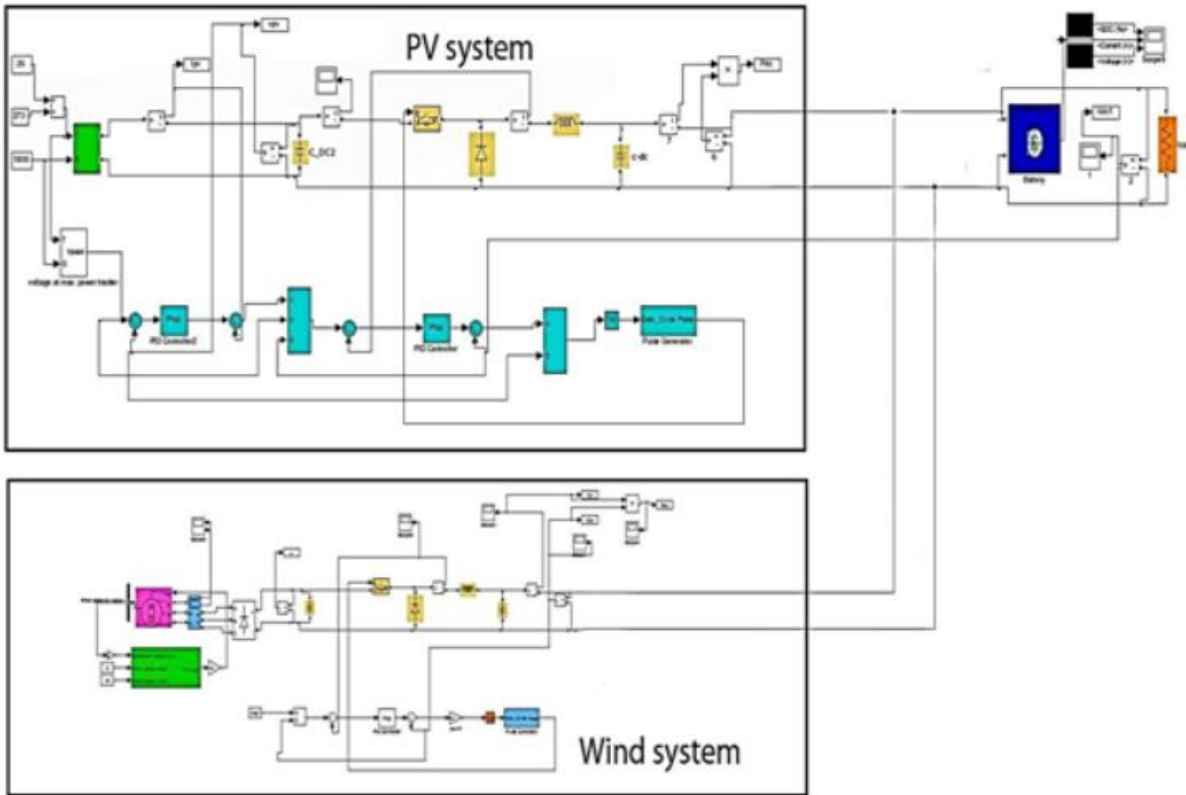

Figure 7: a schematic illustration of an independent hybrid structure

5.0 Simulation results

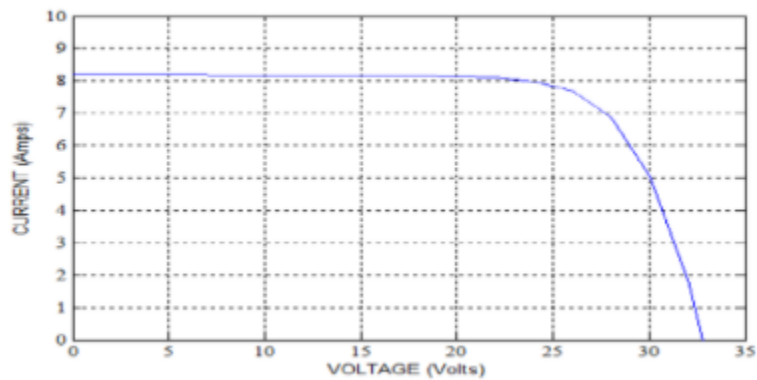Outcomes from a simulation of the photovoltaic (PV) modules.

Figure 8 illustrates the voltage-current curve of a photovoltaic (PV) modules.
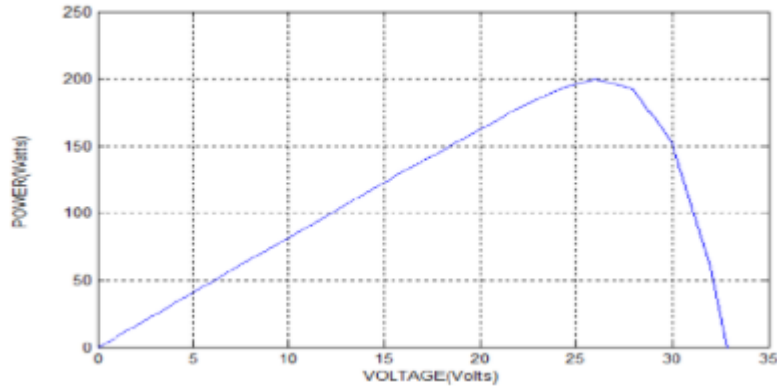
Figure 9 illustrates the P-V curve of a photovoltaic (PV) modules.

Figure 8 and 9 depict the current-voltage (I-V) and power-voltage (P-V) characteristics of a photovoltaic (PV) module. Fig. 8 illustrates that the short circuit current (Isc) of the PV module is around 8.5A, whereas the open circuit voltage (Voc) is roughly 33.2 volts. By examining figure 9, we can deduce that the highest power output is around 210W. This occurs when the current is approximately 7.69A and the voltage at that point is roughly 26.8V.
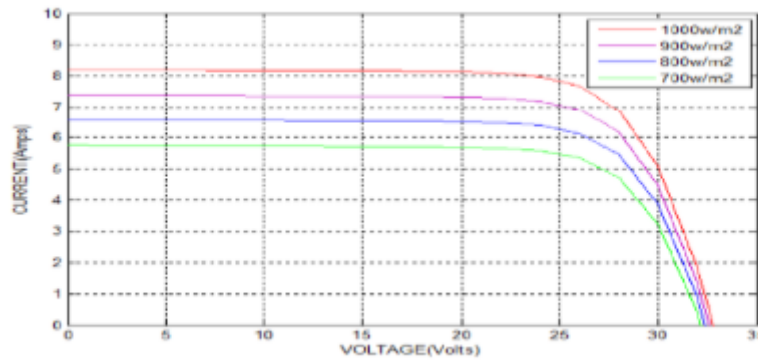
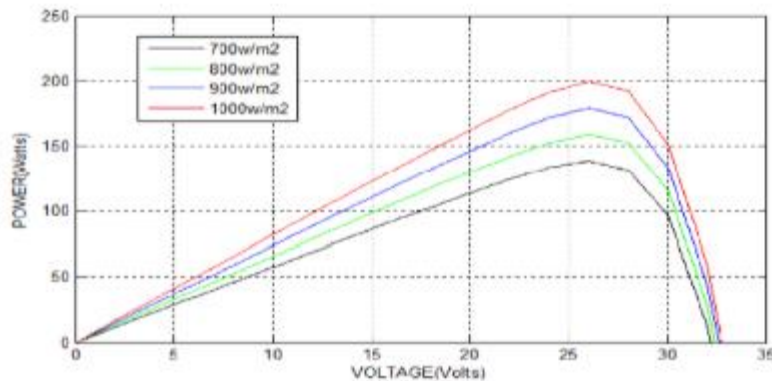Figure 10 illustrates the impact of changes in irradiance on the I-V properties.

Figure 11 illustrates the impact of changes in radiation on P-V properties.

Figures 10 and 11 illustrate the impact of variations in sun irradiation on the properties of photovoltaic systems. Figure 11 illustrates the impact of changes in solar irradiation on the P-V

(power-voltage) characteristics. As the amount of solar radiation increases, the amount of power created also increases. The primary factor contributing to the increase in power is the rise in electric current. By examining figure 10, we can see that there is a direct correlation between the rise in solar irradiation and the increase in short circuit current. The impact of sun irradiation mostly affects the current, as demonstrated in figure 10. As we raise the irradiation from 750 w/m2 to 1050 w/m2, the current increases from roughly 5.7A to 8.2A. However, the influence of solar irradiance fluctuation on voltages is minimal.
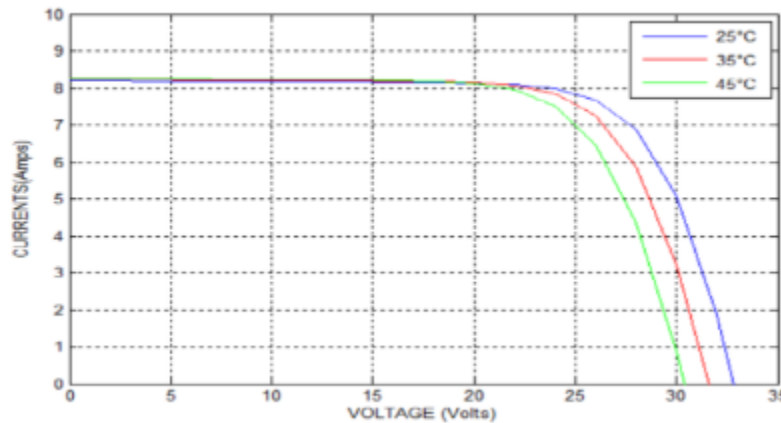
Impact of variations in temperature

Figure 12 illustrates the impact of temperature fluctuations on the I-V parameters.

A rise in temperatures leads to a drop in energy production due to a corresponding fall in voltage. The effect of temperature change on the current-voltage (I-V) characteristics is seen in Figure 12. The figure 12 illustrates that temperature mostly impacts voltage, with a rise in heat resulting in a decline in voltages. However, the present state remained relatively unchanged. Figure 13 illustrates the impact on temperature fluctuations on the P-V properties.
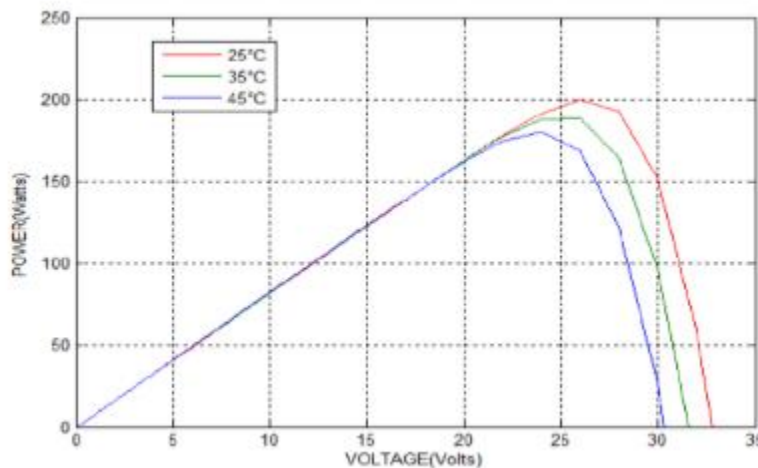

Figure 13 illustrates the impact on temperature fluctuations on the P-V properties
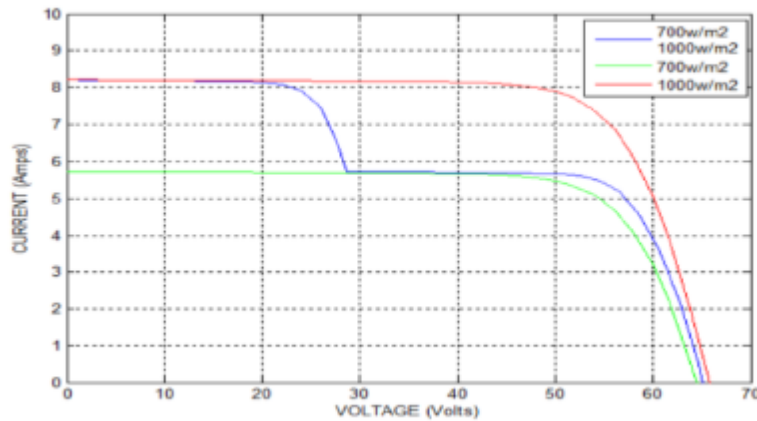
Impact of shading on photovoltaic (PV) arrays.

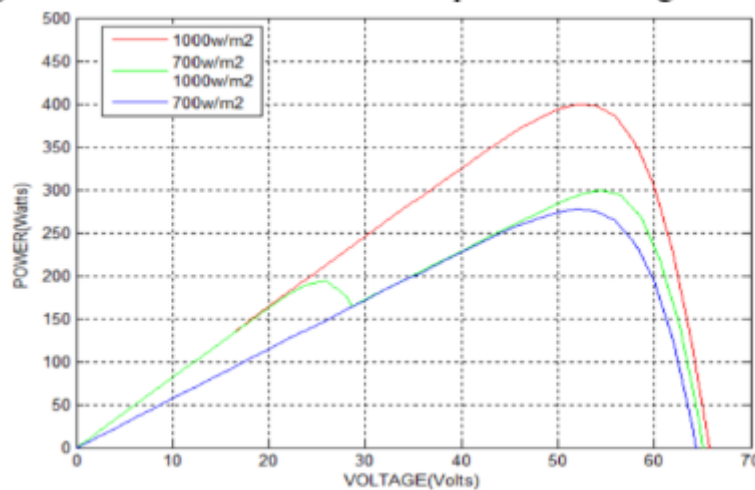Figure 14 illustrates the features of V-I under partial shading conditions.

Figure 15 depicts the P-V parameters under partial shading circumstances.

When there is a small amount of we can see many peaks of the greatest power from figure 15. The current-voltage (I-V) and power-voltage (P-V) characteristics of a photovoltaic (PV) array under shading conditions are depicted in Figure 14 and Figure 15, respectively. Figure 15 demonstrates that partially shaded PV modules provide a lower current compared with an unshaded modules.

Results obtained during Maximum Power Point Tracking (MPPT)

The values shown in Figures sixteen and seventeen show the output power and output voltage, respectively, following the highest possible power point tracking. By referring to figure 16, it is evident that the maximum power, estimated to be about 210 watts, can be monitored. From the data shown in Figure 9, it is evident that the highest power production is attained at a voltage of 26.7 volts. Similarly, Figure 17 demonstrates our ability to accurately monitor and maintain the output voltage at the level that yields the most energy, which is around 26.7 voltages.
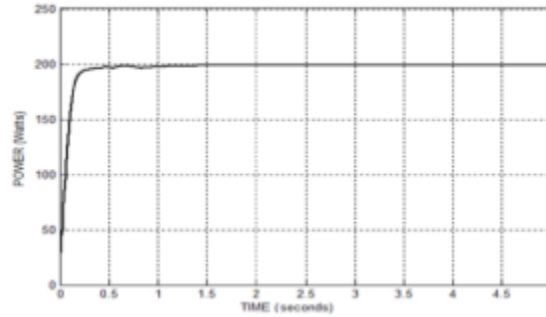
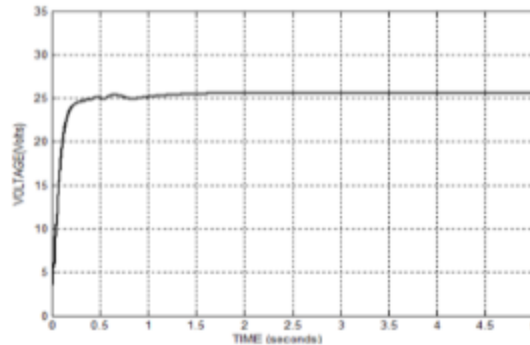Figure 16 displays the power output of the photovoltaic (PV) module after maximum power point tracking (MPPT).

Figure 17 displays the voltage produced by the photovoltaic (PV) module after maximum power point tracking (MPPT) has been applied.

Wind energy system simulation findings

Figure 18 illustrates the power characteristics of a turbine at various wind speeds. By examining Figure 18, it is evident that there is a direct correlation between wind speed and turbine power generation, meaning that as the the breeze speed rises, the turbine's output power likewise rises.
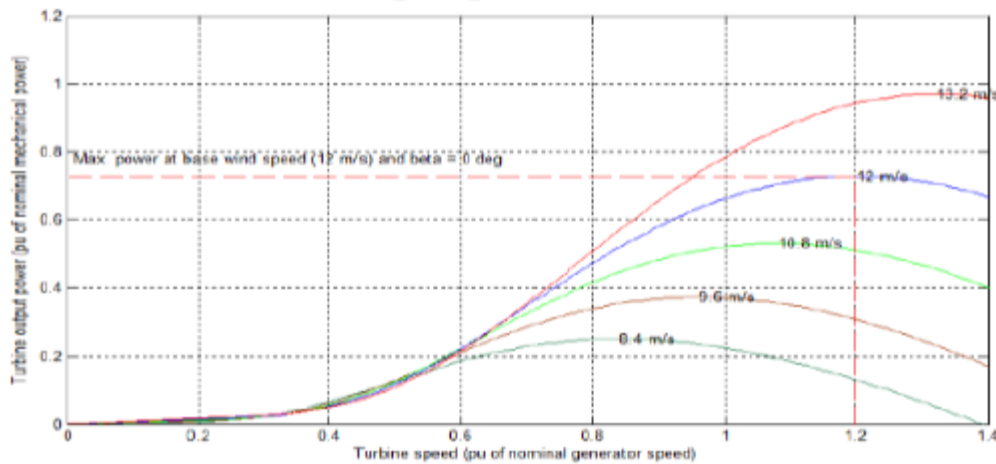

Figure 18 displays the power features of a turbine with an inclined angle of 0°.
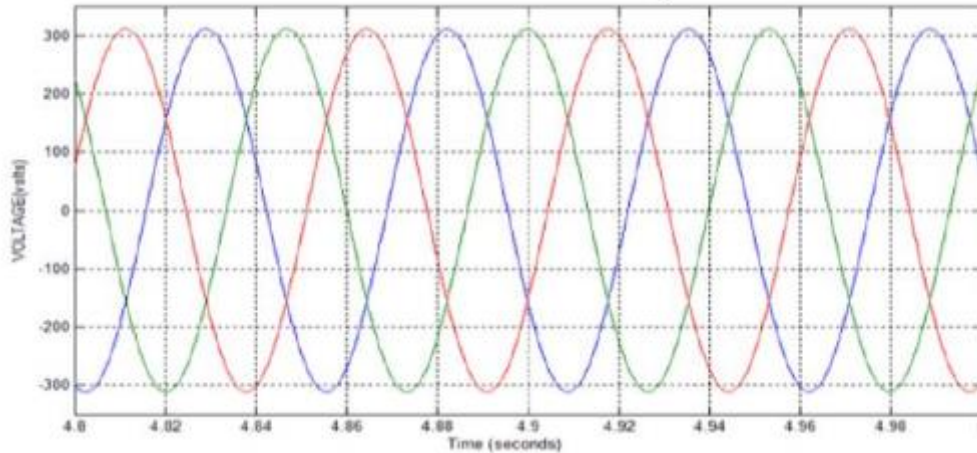
Figure 19 displays the output amplitude for an a three-phase line for a Permanent Magnet Synchronous Generator (PMSG).

The figure 21 displays the output voltage of the wind generator at which the greatest amount of power is attained. The figure 19 displays the PMSG output.The figure 20 above illustrates the location of the highest point of power tracking system, which traces the point of operation of crest power output from the wind generating.
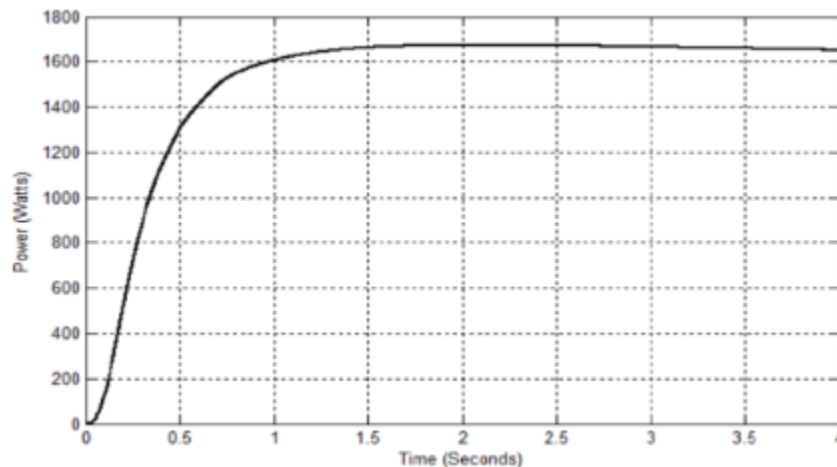

Figure 20 displays the power output of the wind system after Maximum Power Point Tracking (MPPT).

7.0 conclusions

The present investigation presents a multi-input system of energy for hybrids wind/solar power plants. A suggested ASIMULINK model for a Wind-PV hybrids generating system includes all the relevant models of the system elements. The storage device is used to sustain either a wind or solar system in order to satisfy the load. Furthermore, the storage system enables both wind and solar power plants to operate simultaneously for an identical output. The mixture of systems will be modeled and simulated using SIMULINK. Diverse outcomes were achieved under varying operational circumstances, and these outcomes were determined to be acceptable. The power requirement is satisfied by the use of a combination of a photovoltaic (PV) arrays, a turbine for wind power, and a battery. Diverse outcomes were achieved under distinct operational circumstances, and these outcomes were deemed acceptable. Each subsystem was also shown to

4386

engage in shared power in line with the findings. This study is quite valuable for the modeling and fundamental analysis of Wind-PV hybrid structures. This model may be employed for the modeling of a Grid linked Wind-PV systems without additional modifications.

References

[1]. M.MAHALAKSHMI, Dr. S. LATHA," modeling, simulations and sizing of photovoltaic/wind/fuel cell hybrid generation system" International Journal of Engineering Science and Technology (IJEST), Vol. 4 No.05 May 2012.

[2]. M.M Hoque , I.K.A Bhuiyan , Rajib Ahmed, A.A. Farooque & S.K Aditya," Design, Analysis and Performance Study of a Hybrid PV Diesel - Wind System for a Village Gopal Nagar in Comilla", Global Journal of Science Frontier Research Physics and Space Sciences Volume 12 Issue 5 Version 1.0 year 2012.

[3]. Alejandro Rolan, Alvaro Luna, Gerardo Vazquez, Daniel Aguilar, Gustavo Azevedo, " Modeling of a Variable Speed Wind Turbine with a Permanent Magnet Synchronous Generator ". IEEE International Symposium on Industrial Electronics (ISlE 2009) Seoul Olympic Parktel, Seoul, Korea July 5-8, 2009.

[4]. Polinder H., de Haan S. W. H., Dubois M. R., Slootweg J., "Basic Operation Principles and Electrical Conversion Systems of Wind Turbines", NORPIE / 2004, Nordic Workshop on Power and Industrial Electronics, Paper 069, Trondheim, Norway, 14-16 June, 2004.

[5]. MittalR., Sandhu K. S.and Jain D. K. "Low voltage ridethrough (LVRT) of grid interfaced wind driven PMSG," ARPN Journal of Engineering and Applied Sciences., 2009, vol. 4, no. 5. Pp. 73-83.

[6]. Dali M., Belhadj, J., Roboam, X. and Blaquiere, J.M. "Control and energy management of a wind photovoltaic hybrid system", Proc. EPE Conference, 2-5 Sept. 2007, pp 1-10.

[7]. Dali M., Belhadj J., Roboam X., "Hybrid solar-wind system with battery storage operating in grid–connected and standalone mode: Control and energy management - Experimental investigation", Energy 35 (2010) 2587- 2595.

[8]. Akhmatov V., "Variable-Speed Wind Turbines with Doubly-Fed Induction Generators Part III: Model with the Back-to-back Converters", Wind Engineering, Volume 27, No. 2, pp 79-91, 2003

[9]. Hansen A.D., Michalke G., "Modelling and control of variable speed multipole PMSG wind turbine", submitted to Wind Energy, 2007.

[10]. Hong-Woo Kima, Sung-SooKimb, Hee-Sang Koa, "Modeling and control of PMSG-based variable-speed wind turbine", Electric Power Systems Research 80 (2010) 46–52.

[11]. I. Altas, A.M.Sharaf, 2007 "A photovoltaic array (PVA) simulation model to use in Matlab Simulink GUI environment." IEEE I-4244- 0632 -03/07.

[12]. Marcelo GradellaVillalva, Jonas Rafael Gazoli, Ernesto RuppertFilho, "Modeling and circuit-based simulation of photovoltaic arrays", 10th Brazilian Power Electronics Conference (COBEP), 2009.

[13]. J. Hyvarinen and J. Karila.New analysis method for crystalline silicon cells.InProc. 3rd World Conferenceon Photovoltaic Energy Conversion, v. 2, p. 1521–1524, 2003.

[14]. E. Koutroulis, K. Kalaitzakis, and V. Tzitzilonis. Development of a FPGA-based system for real-time simulation of photovoltaic modules. Microelectronics Journal, 2008.

[15]. Geoff Walker. Evaluating MPPT converter topologies using a matlab PV model.Journal of Electrical & Electronics Engineering, Australia, 21(1), 2001.

[16]. W. De Soto, S. A. Klein, and W. A. Beckman. Improvement and validation of a model for photovoltaic array performance.Solar Energy, 80(1):78–88, January 2006.

[17]. Glass.M.C., "Improved solar array power point model with SPICE realization," in Proc. 31st Intersoc. Energy Convers.Eng.Conf. (IECEC), 1996, vol. 1, pp. 286–291.

[18]. Kuo.Y.C., Liang.T.J. andChen.J.F., "Novel maximumpower-point tracking controller for photovoltaic energy conversion system," IEEE Trans. Ind. Electron., 2001, vol. 48, no. 3, pp. 594– 601.Conclusion